Open Archive Toulouse Archive Ouverte (OATAO)

OATAO is an open access repository that collects the work of Toulouse
researchers and makes it freely available over the web where possible

This is an author's version published in: http://oatao.univ-toulouse.fr/27599

Official URL: https://doi.org/10.5006/3199

Chemical interaction of Austenitic and Ferritic Steels with B$_4$C Powder in Liquid Sodium at 600 °C

Marie Romedenne
CEA Saclay
Den-Service de la Corrosion et du Comportement des Matériaux dans leur Environnement (SCCME), CEA, Université Paris-Saclay, F-91191, Gif-sur-Yvette
France
Fabien Rouillard
CEA Saclay
Den-Service de la Corrosion et du Comportement des Matériaux dans leur Environnement (SCCME), CEA, Université Paris-Saclay, F-91191, Gif-sur-Yvette
France
Didier Hamon
Den-Service de Recherches Métallurgiques Appliquées (SRMA), CEA, Université Paris-Saclay, F-91191, Gif-sur-Yvette
France
Michel Tabarant
Den-Service d'Etudes Analytiques et Réactivité des Surfaces (SEARS), CEA, Université Paris-Saclay, F-91191, Gif-sur-Yvette
France
Daniel Monceau
CIRIMAT, Université de Toulouse, CNRS, INPT, UPS, ENSIACET 4, allée Emile Monso BP-44362
31030 Toulouse cedex 4
France

ABSTRACT

In the framework of studies on the control rods lifetime for the Sodium Fast Reactor prototype development, three commercial steels were exposed to B$_4$C powder in sodium at 600 °C for durations up to 3000 h. Analyses by optical and secondary electron microscopy, electron microprobe and glow discharge optical emission spectrometry revealed the formation of borides layers on the steel surface and slight carburization deeper in the steels. The growth of the boride layers followed parabolic kinetics. The natures of the formed boride layers were in good agreement with thermodynamic equilibrium predicted by Thermo-Calc software. The carburization depths were much lower than the ones obtained in pure carburizing sodium at 600 °C. It did not grow with time revealing possible protective character of the boride layers against carbon penetration.

Keywords: Carburization, Boriding, Steels, Sodium

INTRODUCTION

In order to preserve uranium natural resources and to decrease the quantity of nuclear waste, France is developing a sodium-cooled fast reactor (SFR) prototype named ASTRID. Currently, research studies are under way to evaluate the control rods lifetime. In the current concept, the control rods are made of B_4C pellets encapsulated in stainless steel clads.[1] Feedbacks from former French SFRs revealed that the control rods lifetime was limited by clad embrittlement likely induced by interaction with B_4C.[2]

With the aim of better understanding this clad embrittlement, out-of-pile exposure of three different candidate steel grades in sodium containing nuclear grade B_4C powder were carried out at 600 °C, the maximum expected temperature in the reactor. The nature of the corrosion products was identified and their kinetics of formation were followed through several exposure times up to 3000 h. Particular attention was given to the carbon and boron concentration profiles through the steel surface as carburization and/or boriding were suspected to be responsible of control rod clad embrittlement in French SFRs.

EXPERIMENTAL PROCEDURE

Three different steel grades, AIM1, 316L and EM10, were exposed to sodium containing nuclear grade B_4C powder for 250, 500, 1000, and 3000 h at 600 °C. In order to avoid any interaction between the different steel grades and to minimize the reaction of B_4C powder with the crucible, the three steel grades were positioned in three single alumina crucibles ; one for each steel grade. Each crucible contained 200 g of sodium with 10 g of B_4C powder which composition is given in Table 1. They were inserted in a large molybdenum crucible with liquid purified sodium. The amount of B_4C put into the crucible was chosen in large excess respect to the expected corrosion kinetics. Before pouring the B_4C powder into the crucibles, the residual oxygen level in sodium was pumped out at 600 °C for three days using large zirconium foil in order to reach an oxygen concentration lower than 5 wppm, in agreement with the level expected in French SFRs.[3] The carbon content in the sodium bath obtained from this experimental procedure was not measured but has been characterized in other studies from our laboratory to be carburizing.[4] In order to evaluate the carburizing character of the used sodium, 316L samples were exposed outside of the crucibles in the molybdenum crucible filled with purified sodium which did not contain any B_4C powder.

Detailed chemical compositions of AIM1 (austenitic and 25% strain-hardened), 316L (austenitic and annealed) and EM10 (ferritic and 25% strain-hardened), used in the present study are given in Table 2. All specimens were parallelepiped (15 * 10 * 1 mm^3) and exposed in their as-received surface finish. After each exposure time, the specimens were cleaned three consecutive times smoothly with ethanol to remove the residual sodium present on their surface and then weighed. Then, one part of the sample was cut and etched with ammonium persulfate (10 g $(NH_4)_2S_2O_8$, 100 mL H_2O, 10 sec, 6 V) or ground and polished down to silicon oxide suspension for optical and secondary electron microscopy examination. Carbon and boron concentration profiles were carried out through the sample's cross section by Electron Probe Micro Analysis (SX 100 CAMECA) at 15 kV and 20 nA. The analytical crystal was LPC2 for Kα C and PC3 for Kα B. Three quantitative profiles (step 4 μm for carbon and step < 1 μm for boron) were carried out over the mid-thickness of each sample and averaged. The obtained relative deviation was 5 %. Since carbon was usually mainly contained into carbides which precipitated in the substrate grain boundaries, the carbon profile was measured through band scan mode which length was larger than twice the austenitic grain size at least (2 x 50 μm²). Carbon and boron were quantified with the phi-rho-z method using SiC and B_4C standards. Despite all precautions, carbon pollution was observed on the surface due to samples' preparation and to carbon deposition in the vacuum chamber under electron beam. The level of pollution was evaluated to be 0.5 wt.% for all steels from the analysis on the initial non-carburized specimen and subtracted to all the carbon profiles. This carbon quantification method has been shown to be quite effective for highly carburized steel samples

in a previous study.[5] Point scan mode (diameter around 1 µm) was used to measure boron concentration. 0.2 wt.% of boron was subtracted to all the boron profiles to adjust the Kα B line position. The carbon and boron concentration profiles were also obtained by Glow Discharge Optical Emission Spectroscopy (GDOES) at 850 Pa and 30 W with Horiba Jobin Yvon GD-Profiler 2. The concentration profiles were performed on a 4 mm diameter area, with a theoretical 2.5 nm depth resolution up to about 20 µm in depth.

Table 1
Composition of HP grade B_4C powder (in wt.%) provided by H.C. Starck

Chemical composition (wt. %)							
C	N	O	Fe	Si	Al	Other	B
21.8	0.7	1.0	0.05	0.15	0.05	0.5	Bal.

Table 2
Composition of the studied steels grades (in wt.%) obtained by Inductively Coupled Plasma-Optical Emission Spectrometry (ICP-OES)

Steel	Chemical composition (wt.%)										
	Cr	Ni	Mo	C	Ti	Mn	Co	Si	Cu	Al	Fe
AIM1	14.35	14.05	1.40	0.09	0.36	1.40	0.02	0.73	0.012	0.015	Bal.
316L	16.55	10.52	2.05	0.03	-	1.55	0.12	0.18	0.24	0.022	Bal.
EM10	8.95	0.42	0.82	0.1	0.013	0.65	0.03	0.33	0.015	0.096	Bal.

RESULTS

1. Evolution of weight gain per unit of area

Figure 1 (A) shows the evolution of the weight gains per unit of area of AIM1, 316L and EM10 steels as function of exposure time. All steel grades gained mass during their exposure revealing interaction with B_4C powder. After 3000 h exposure, the mass gains were between 1.1 and 1.4 mg.cm^{-2}, the highest being for 316L steel. Furthermore, as shown in Figure 1 (B), the weight gain per unit of area followed parabolic kinetics for the three steels revealing a diffusion-controlled phenomenon.
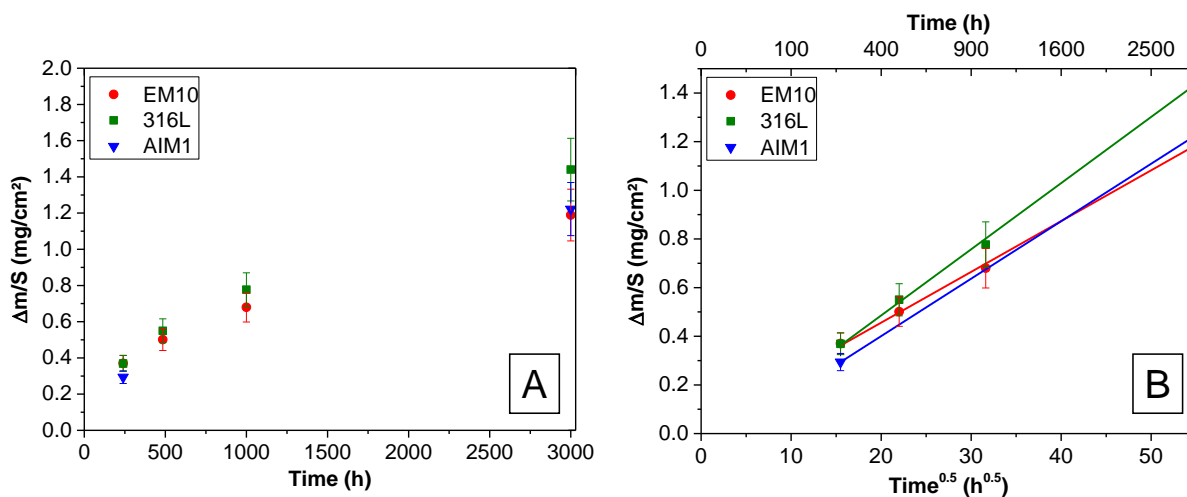

Figure 1 : (A) Measured mass gain per unit of area of AIM1, 316L and EM10 as a function of exposure time in liquid sodium with B_4C powder at T = 600 °C.
(B) Corresponding parabolic plots.

2. Surface characterization

a. Optical examination

The etched cross-section samples after 1000 h exposure are shown in Figure 2. Three distinct zones were identified and are represented in Figure 2. Zone 1 was made of a continuous corrosion layer formed on the steel surface, zone 2 corresponded to the zone where grain boundaries were strongly corroded and zone 3 was assigned to long range grain boundary diffusion.
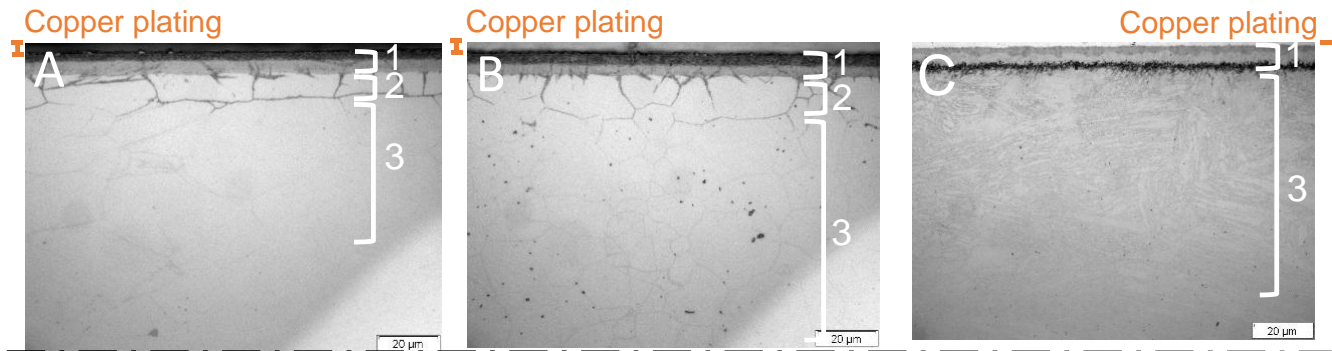

Figure 2 : Images of the revealed borided and carburized layers for (A) AIM1, (B) 316L and (C) EM10 after 1000 h exposure observed by optical microscopy.

b. Nature of the identified zones

The chemical nature of the identified zones was determined using WDS X-ray mapping then quantified through profiles obtained by GDOES and EPMA. WDS X-ray mapping of 316L cross-section sample after 1000 h exposure showed the formation of a surface duplex boron enriched corrosion layer (Figure 3). For the three steels GDOES analysis of this layer demonstrated that the outer and the inner layer were enriched with 45 ± 5 at.% and 30 ± 3 at.% of boron respectively (Figure 4, Figure 5 and Figure 6). These concentration values were confirmed by EPMA measurements. These measured atomic concentrations suggested that the corrosion zone identified by zone 1 in Figure 2 were formed of MB and M_2B borides in the outer and inner layers respectively. The same corrosion layers were observed on the other steel grades (Figure 5 and Figure 6). It was observed that the thicknesses of the boride layers increased with time as reported in Table 3. The values in Table 3 corresponded to an average of twenty five measurements for each boride layers. Moreover, the MB thickness over M_2B thickness ratio increased with time. For AIM1, the MB thickness was roughly equal to the M_2B thickness after 3000 h exposure. This value was reached for 316L at shorter time exposure after 500 h and staid quite constant at longer times. GDOES profiles shown in Figure 4, Figure 5 and Figure 6 were quite efficient to measure any enrichment or depletion of elements through the surface. For the three steel grades, they revealed that the two boride layers contained the main metallic elements of the substrate, Fe, Cr and Ni in atomic concentrations roughly equal to the substrate's ones. Nevertheless, by looking more carefully, slight chromium enrichment followed by nickel enrichment underneath could be observed in the outer part of MB (first 2 µm) for the three steel grades. Furthermore, the inner M_2B boride layer might be slightly depleted in nickel compared to iron and chromium. Finally, it was interesting to note that nickel depletion in the substrate underneath the boride layers was detected. This phenomenon with the observation of nickel precipitates on top of the boride surface, for both austenitic steels (Figure 4 and Figure 5), suggested nickel dissolution in sodium then reprecipitation onto the sample surface.

Carbon concentration profiles were obtained by GDOES for short-range depth profiles and by EPMA for long-range depth profiles. No carbon was detected in the duplex boride layer formed on AIM1 and EM10 steels after any exposure time (Figure 4 and Figure 5). Moreover, on these same steels, a carbon enrichment zone characterized by a diffusion profile was detected deeper in the steel. This carburized zone is identified as zone 3 in Figure 2. Its maximum depth reached 250 and 150 µm for

AIM1 and EM10 steels respectively after 250 h. Interestingly, this carburization depth did not grow with time (Figure 7). For AIM1 steel, the highest value of carbon concentration observed in Figure 7, were induced by the presence of large band of Ti carbides which had precipitated along the rolling direction during steel making. The carbon enrichment in the substrate was detected immediately underneath the boride layer for EM10 but much deeper for AIM1. Indeed, as shown in Figure 4, the carbon concentration within the first twenty microns underneath the boride layer formed on AIM1 was much lower than the initial carbon content revealing carbon depletion. This carbon depletion depth was in good agreement with what is called zone 2 in Figure 2 where large intergranular boride precipitates were formed.

The carbon profile in 316L steel was quite different from the other steel grades. Carbon enrichment was observed in the duplex boride layer and underneath it, in the metallic substrate. The carburization zone depth reached 200 µm after 250 h and, again, did not grow with time. It was characterized by the formation of carbides into grain boundaries (Figure 3).

The penetration depths of zone 2 and 3 were measured as a function of exposure time and reported in Table 3. For the three steels, the identified zones 1 to 3 are displayed in Figure 8 on cross section electronic images after etching.

Table 3
Evolution of the thicknesses of the three identified zones

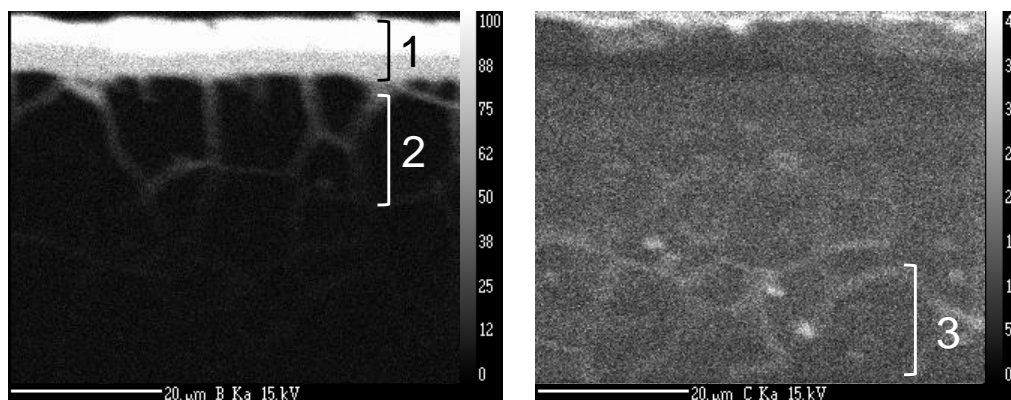|		AIM1 (µm)	316L (µm)		EM10 (µm)
Zone 1 – MB layer	250 h	0	0.9 ± 0.1	Zone 1 – MB + M$_2$B layers	2.9 ± 0.3
	500 h	0.7 ± 0.1	2.7 ± 0.2		4.6 ± 0.3
	1000 h	2.4 ± 0.2	3.2 ± 0.2		7.0 ± 0.6
	3000 h	6.7 ± 0.4	7.9 ± 0.5		11.0 ± 1.3
Zone 1 – M$_2$B layer	250 h	2.6 ± 0.2	1.2 ± 0.2		
	500 h	3.4 ± 0.3	2.5 ± 0.3		
	1000 h	4.7 ± 0.5	3.6 ± 0.3		
	3000 h	7.2 ± 0.4	6.1 ± 0.6		
Zone 2	250 h – 3000 h	20 - 30	15 – 25	Zone 2	0
Zone 3	250 h – 3000 h	200	250	Zone 3	150

Figure 3 : WDS X-ray mapping of boron (left) and carbon (right) of 316L steel surface after 1000 h exposure in liquid Na with B$_4$C powder at 600 °C.
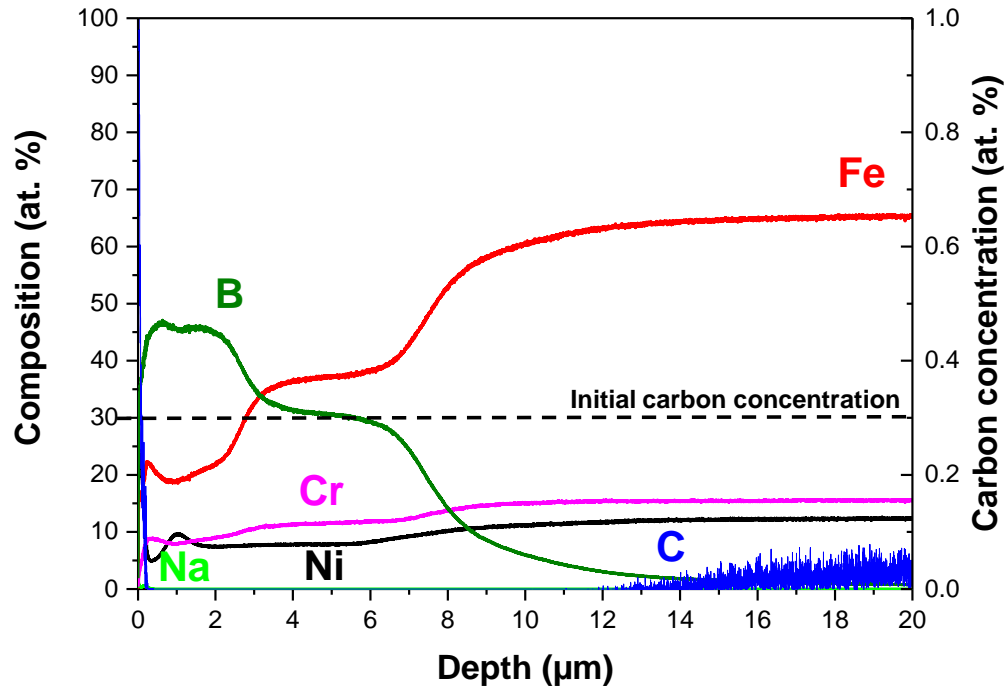
Figure 4 : GDOES concentration profiles for AIM1 steel as a function of depth after 1000 h exposure to B$_4$C powder and liquid Na at 600 °C.
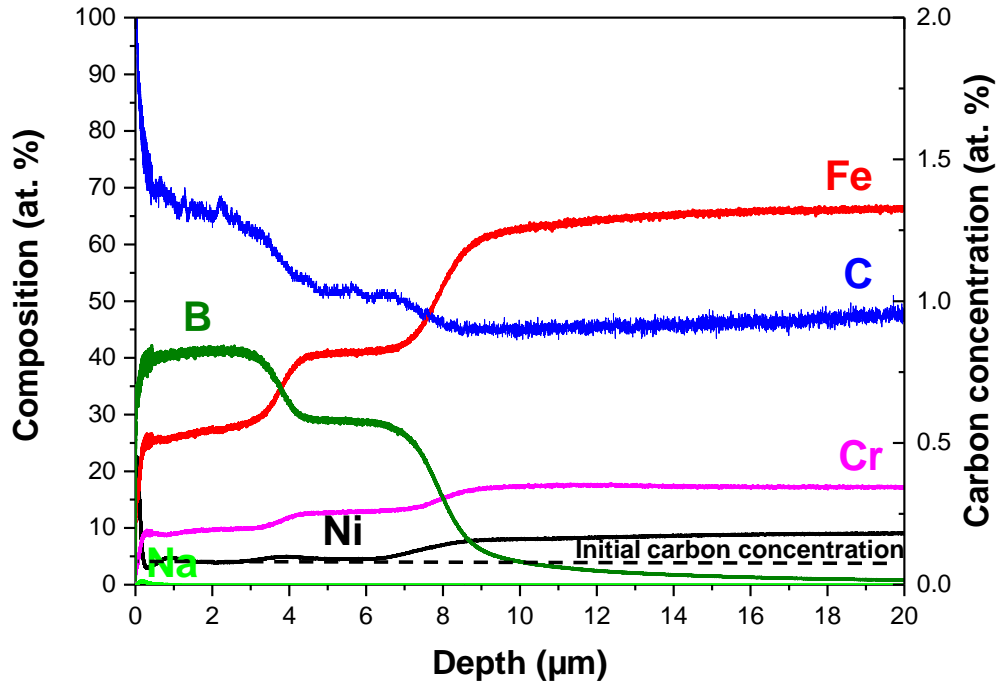
Figure 5 : GDOES concentration profiles for 316L steel as a function of depth after 1000 h exposure to B$_4$C powder and liquid Na at 600 °C.
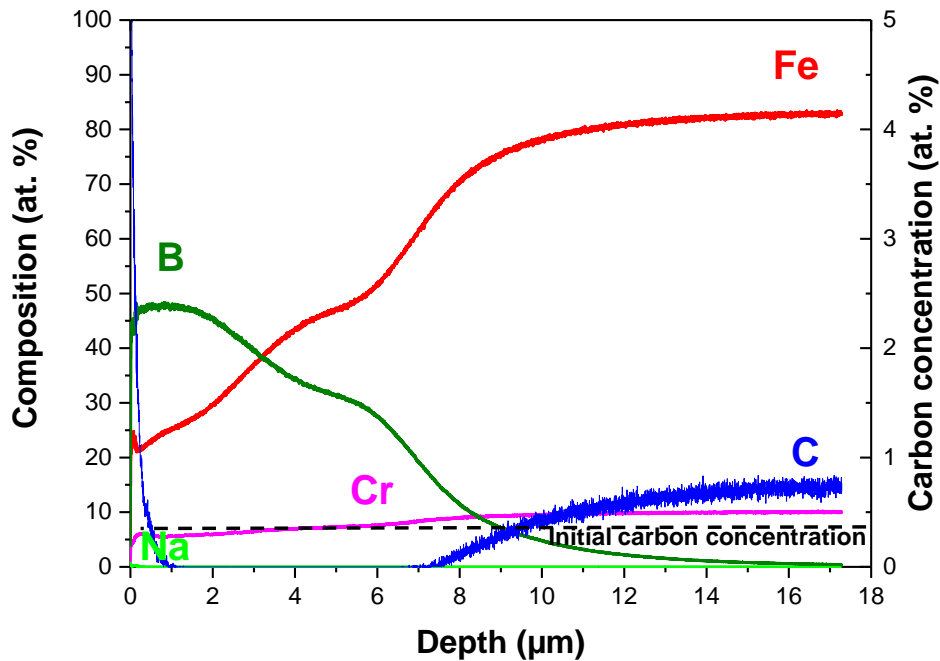

Figure 6 : GDOES concentration profiles for EM10 steel as a function of depth after 1000 h exposure to B$_4$C powder and liquid Na at 600 °C.
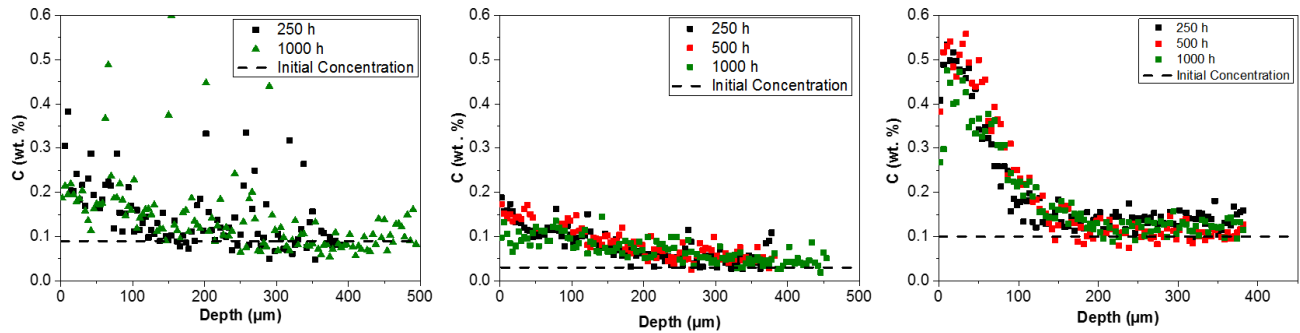
Figure 7 : EPMA carbon concentration profiles for (A) AIM1, (B) 316L and (C) EM10 steels as function of depth after 250 h, 500 h, and 1000 h exposure in liquid Na containing B$_4$C powder at 600 °C.
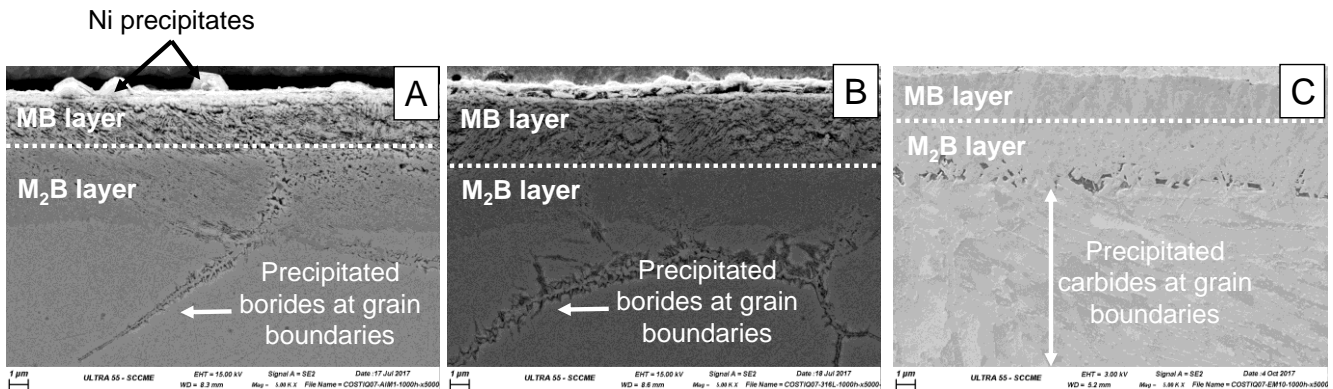

Figure 8 : Images of the revealed borided and carburized layers for (A) AIM1, (B) 316L and (C) EM10 after 1000 h exposure observed by SEM.

DISCUSSION

1.   Nature of the chemical interaction

The three studied steel grades, in contact of B$_4$C powder in sodium at 600 °C, formed a duplex boride layer, MB and M$_2$B. The formation of these two layers was also identified by XRD by Heuvel *et al.*[6] after exposure of X10CrNiMoTiB1515 and X8CrNiMoNb1616 with B$_4$C pellets in liquid sodium at the same temperature, 600 °C for 1000 h. M$_2$B phase was the only phase characterized by Chandran *et al.*[7] after exposure of 15Cr15Ni (D9 steel) steel with B$_4$C pellets in liquid sodium at higher temperature, 700 °C. The growth kinetics of these two layers was characterized to be parabolic which suggest a diffusion controlled growth process and within the 3000 h exposure, the growth kinetics of MB was shown to be higher than M$_2$B.

Besides, the three steel grades were observed to carburize slightly underneath the boride layer. The amount of carbon injected in the substrate was around 100 times higher than the amount of carbon which could had been explained by the dissociation of carbides initially present in the boride layers followed by carbon back-diffusion deeper into the substrate as proposed by Heuvel *et al.*[6] Thus, carburization of the steels from the sodium occurred. Nevertheless, the fact that the carburization profile reached after 250 h exposure did not evolve with time for the three steel grades suggested strongly that this carburization phenomenon was only transient during the initial exposure stage. It could be explained by the initial carburizing character of sodium before the dissolution of B$_4$C powder in it. Then, once B$_4$C had sufficiently dissolved in sodium to form a boride layer on the steel surface, the carbon penetration into the metallic substrate stopped. Differently from the two other steel grades,

carbon was detected as well in the boride layer formed in 316L. The form under which carbon was present in the boride layer was not known but it might be stable chromium carbides which were formed during the transient stage and which did not dissolved entirely during the following formation of the boride layer. The carburization of austenitic steels in sodium containing B_4C was also revealed by Chandran *et al.*[7] at 700 °C. They affirmed that carbon came from the dissolution of B_4C but this conclusion may be an early conclusion since nuclear grade sodium is usually carburizing as well. Heuvel et al.[7] in their study at 600 °C, revealed the formation a carburization zone underneath the boride layer but affirmed that the excess of carbon came from the initial carbon contained in the borided zone only. From our study, it is believed that both initial carbon present in nuclear grade sodium and carbon from B_4C powder explained the additional carbon measured underneath and into the boride layer. Although the steels were carburized after exposure with B_4C powder, their carburization degree and the total carburization depths were much lower than the ones obtained in highly carburizing sodium in a previous study at 600 °C.[5]

2.   Thermodynamics

Thermo-Calc software was used with TCFE8 database to calculate the phases formed at thermodynamic equilibrium in the steels under the presence of boron and carbon. Calculations were performed at 600 °C with Fe, Cr, Ni and C compositions given in Table 2 for the three steel grades. No major difference with respect to the phases which could be formed on AIM1, 316L and EM10 was observed. In order to evaluate if the preferential formation of surface boride layers at the expense of carbides could have been predicted in these experiments, the carbon and boron activities in the environment were calculated and compared to the ones needed for the formation of metallic borides and carbides. Figure 9 shows that borides are much more stable than carbides (a_B needed to form M_2B activity is about three order of magnitude lower than a_c needed to form $M_{23}C_6$). Nevertheless, careful attention should be paid before giving conclusions at this stage since carbon and boron activity reached in sodium depends on the solubility of boron and carbon in sodium.

The carbon and boron activities were calculated using Equation (1), where $S_{C,B}(Na)$ is the solubility of carbon[8] or boron[9] in sodium. Assuming stoichiometric dissolution of B_4C in liquid sodium and using Equation (1), a relation between a_B and a_c was calculated in Equation (2). From this assumption, a_B was calculated equal to 0.2 times a_C. The solubility of carbon, $S_C(Na)$, is well documented.[8] Its value was 5.5 ppm at 600 °C. But the boron solubility, $S_B(Na)$, is not well described in literature[9]. In order to evaluate the boron activity in Na, minimum and maximum values were calculated. The minimum value of $S_B(Na)$ was taken equal to $S_C(Na)$ since it has been proposed that boron was more soluble than carbone.[9] The maximum value was calculated using the proposed value given by Adams *et al.* at 500 °C[10], 20 ppm, and assuming that the solubility difference between carbon and boron at 500 °C was kept at 600 °C. A maximum value of 148 ppm was taken for $S_B(Na)$. According to these assumptions, the boron and carbon activity ranges which might have been obtained in sodium are plotted in Figure 9. From all these assumptions, the formation of M_2B and MB layers on all steel grades when exposed in sodium containing B_4C were predicted thermodynamically, in good agreement with what was observed experimentally.

$$a(B \text{ or} C) = \frac{[C \text{ or } B]}{S_{C,B}(Na)} \qquad (1)$$

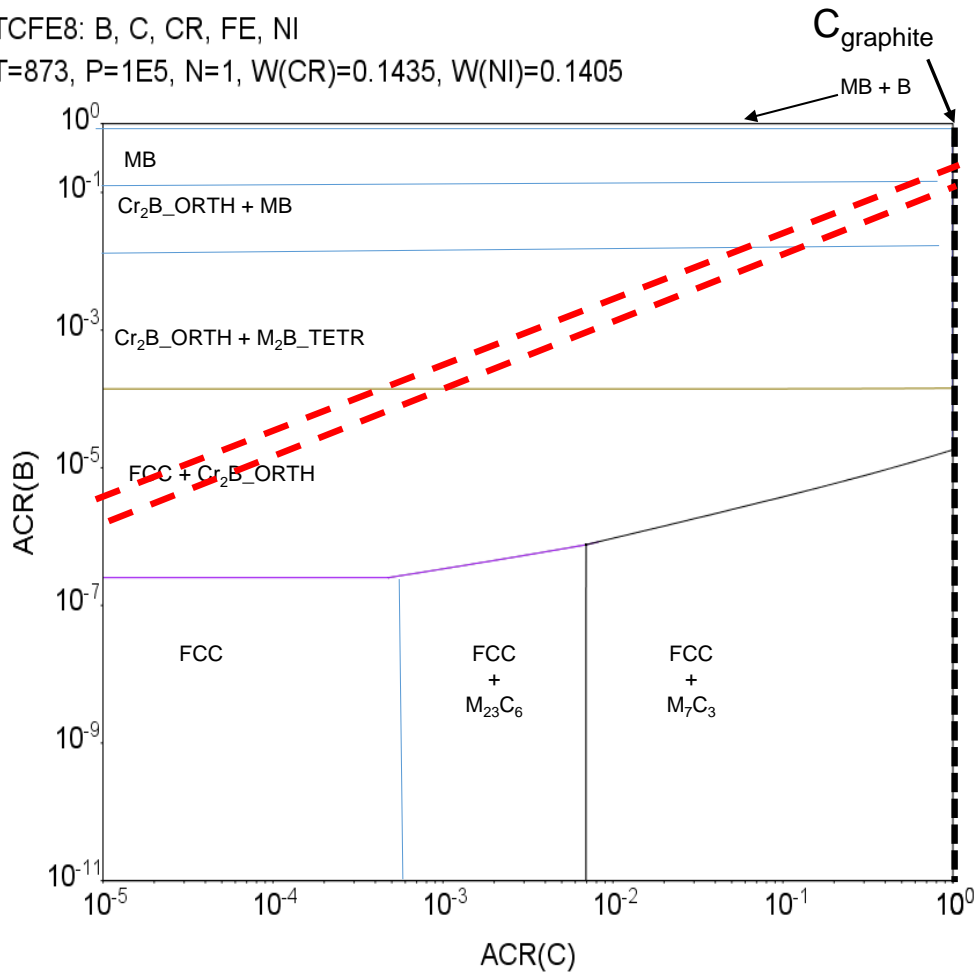$$a_B = \frac{4S_C(Na)a_C}{S_B(Na)} \qquad (2)$$

Figure 9 : ThermoCalc predominance diagram for AIM1 steel at 873 K with Fe, Cr, Ni, C composition and TCFE8 database with boron activity range reached in sodium.

3. Kinetics

Parabolic rate constants of the boride layer growth, k_p, were determined using Equation (3), where x_i corresponded to the total boride thickness measured using SEM images and t, the exposure time.

$$x_i^2 = k_p t \qquad (3)$$

This method led to respective parabolic rates for the total boride layer of $1.9 \ 10^{-13}$ cm².s⁻¹ for AIM1 and 316L steels and of $1.1 \ 10^{-13}$ cm².s⁻¹ for EM10 steel. The experimental k_p are plotted in Figure 10. The parabolic rate constants were in accordance with an extrapolation of Chandran *et al.*[7] values obtained at higher temperature assuming that the activation energy was equal to the one calculated by Heuvel *et al.*[6] However, the k_p were ten times lower than the kinetics law calculated by Heuvel *et al.*[6] Both authors used a different configuration than the one used in our study. They used B_4C pellet inserted in steel clads. The discrepancy between the k_p values obtained by both authors is difficult to explain. The observation that the parabolic constant of boride formation with B_4C powder is roughly equal to the extrapolated one from Chandran *et al.'s*[7] and Heuvel *et al.*[6] studies with B_4C pellet suggested low

influence of the geometrical aspect of B_4C. More work is, nevertheless, needed to confirm this tendency.

From our study, a total boride layer thickness equal to 50 µm at 600 °C could be expected after four years, the targeted control rod lifetime for the French SFR prototype. The influence of this layer thickness as well as the influence of intergranular boride formation and carburization on the mechanical properties should be evaluated.
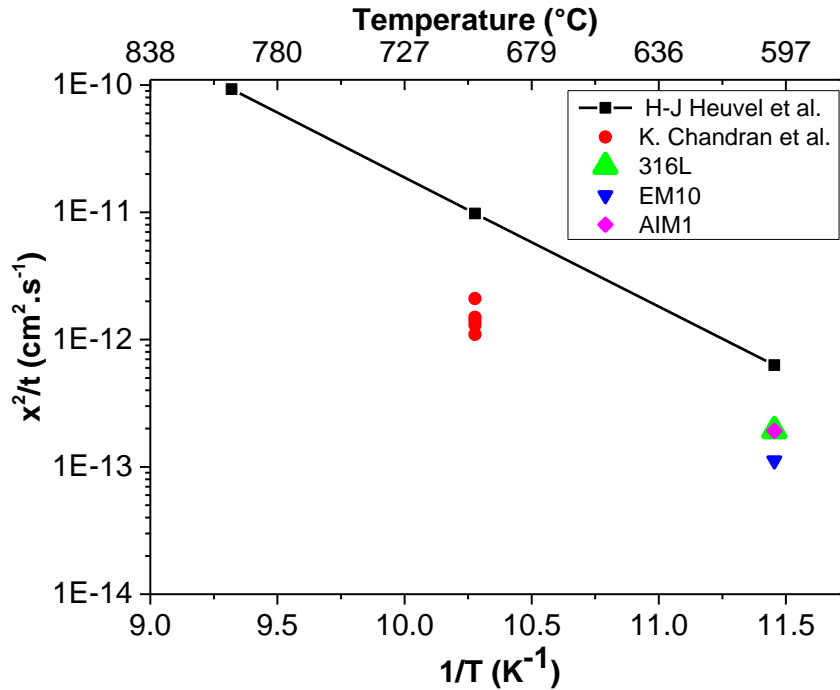

Figure 10 : Parabolic rates constant plotted in function of the inverse temperature and compared with literature data [6, 7]

CONCLUSIONS

At 600 °C, it has been demonstrated that the B_4C powder dissolved in liquid sodium and reacted with the steels to form two boride layers at the surface and a carburized zone underneath. The composition of the boride layers lead to the conclusion that M_2B and MB layers were formed at the surface of the steels with M = Fe, Cr and Ni mainly. Carburization of the steels was observed and might have been formed during the transient stage when boron dissolution was low and sodium was mainly carburizing, or before the formation of a continuous boride layer. The carburization degree and carburization depths of the steels were much lower than the ones obtained in highly carburizing sodium observed in a previous study at 600 °C.[5] Complementary experiments are needed to understand the evolution of the chemical interaction between the B_4C powder and the steels. Furthermore, tensile test will be done to study the impact of the boro-carburization on the mechanical properties of the steels.

ACKNOWLEGMENTS

REFERENCES

1.   Escleine, J.M. and S. Lansiart, *L'aiguille « absorbante » des cœurs rapides français. Un point sur la conception, la modélisation et les moyens de calcul – Perspectives*. 2008, CEA.

2.   Rouillard, F., M. Romedenne, and D. Gosset, *"Etat de l'art sur l'interaction B₄C – acier de gaine et loi de durée de vie des gaines des éléments absorbants"*. 2017, (Saclay, France : CEA).

3.   Guidez, J., *Phénix le retour d'expérience*. (France: EDP Sciences, 2013). p. 225.

4.   Hémery, S., T. Auger, J.L. Courouau, and F. Balbaud-Célérier, "Effect of oxygen on liquid sodium embrittlement of T91 martensitic steel." *Corrosion Science*, 76(2013): p. 441-452.

5.   Romedenne, M., F. Rouillard, B. Duprey, D. Hamon, M. Tabarant, and D. Monceau, "Carburization of Austenitic and Ferritic Steels in Carbon-Saturated Sodium: Preliminary Results on the Diffusion Coefficient of Carbon at 873 K." *Oxidation of Metals*, 87(2017): p. 643-653.

6.   Heuvel, H.J., P. Holler, and P. Dunner, "Absorber material cladding chemical interaction in vented fast breeder reactor absorber pins - B4C stainless steel chemical interaction in sodium environment and effect of metallic Nb and Cr layers." *Journal of Nuclear Materials*, 130(1985): p. 517-523.

7.   Chandran, K., S. Anthonysamy, M. Lavanya, R. Sudha, P.R. Reshmi, D. Annie, R.R. Madhavan, T.N. Prasanthi, C. Sudha, S. Saroja, and V. Ganesan, *Studies on the Chemical Compatibility of Alloy D9 with B4C in The Presence of Sodium*, in *Structural Integrity*, T. Jayakumar, et al., Editors. 2014, Elsevier Science Bv: Amsterdam. p. 631-638.

8.   Thompson, R., *Carbon Solubility and Solute species in Liquid Sodium*. 1980, AERE, Harwell, Oxon, United Kingdom

9.   Borgstedt, H.U. and C. Guminski, "IUPAC-NIST solubility data series. 75. Nonmetals in liquid alkali metals." *Journal of Physical and Chemical Reference Data*, 30(2001): p. 835-1156.

10.   Adams, P.F., *Ph. D. Thesis, University of Nottingham, U.K, 1977; abstracted in C. C. Addison, The Chemistry of the Liquid Alkali Metals (Wiley, Chichester, 1984)*. p. 225.